# Electrical Behavior of an Ultralow-Energy Plasma-Focus Device

Mario Oscar Barbaglia, Horacio Bruzzone, Hugo Néstor Acuña, Leopoldo Soto, and Alejandro Clausse

***Abstract*— Measurements of electrical signals in discharges performed in a miniature plasma-focus device (5 nF capacitor bank, central electrode diameter and effective free length 2.0 and 0.5 mm, respectively, no outer electrode) are reported. A lumped model is built that gives good agreement between the model and the recorded signals. The main conclusions are as follows: the voltage at which the chamber disk capacitor is charged is limited by the gas filling pressure inside the chamber and not just by the voltage in the capacitor energy source, and the behavior of the discharge current within the vacuum chamber depends on the whole system and not only on the last portion of the circuit, even for longer transmission line lengths.**

***Index Terms*— Fusion reactors, plasma devices, plasma focus.**

## I. Introduction

PLASMA-FOCUS (PF) devices are known to be efficient sources of short bursts of hard and soft X-rays, neutrons, and ions, as well as electron beams [1]. Because of the fact that these devices have unique qualities such as low cost, compact size, and low operation risk (compared with isotopic neutron sources), they are potential candidates to replace standard radioactive nuclear sources.

Recently, some studies have been made on a device operating in a PF-like configuration involving an astoundingly small driving energy [2], [3] in the order of tenths of a joule. This device uses a coaxial electrode geometry without a surrounding electrode (i.e., the cathode is simply the vacuum chamber back plate), a configuration that was previously studied by others [2], [4]–[6]. However, in the present case the system is powered by a rather unconventional circuit whose functioning is not obvious and deserves some additional study. In this paper, an analysis of this circuit is presented together with some measurements performed in one of these devices currently operating in Argentina, in order to obtain a better understanding of its electrical behavior.

Manuscript received June 1, 2013; revised September 12, 2013 and October 29, 2013; accepted December 1, 2013. Date of current version January 6, 2014. The work of L. Soto was supported by FONDECYT-Chile under Grant 1110940.

M. Barbaglia is with CONICET and Universidad Nacional del Centro, Tandil 7000, Argentina (e-mail: barbagli@exa.unicen.edu.ar).

H. Bruzzone and H. Acuña are with the Universidad Nacional de Mar del Plata and CONICET, Mar del Plata 7600, Argentina (e-mail: bruzzone@mdp.edu.ar; hacuna@mdp.edu.ar).

L. Soto is with Comision Chilena de Energía Nuclear and Center for Research and Applications in Plasma Physics and Pulsed Power P4, Santiago 188-D, Chile (e-mail: lsoto@cchen.cl).

A. Clausse is with CONICET and Universidad Nacional del Centro, Tandil 7000, Argentina, and also with the National Atomic Energy Commission, Buenos Aires 6154, Argentina (e-mail: clausse@exa.unicen.edu.ar).

Color versions of one or more of the figures in this paper are available online at http://ieeexplore.ieee.org.

Digital Object Identifier 10.1109/TPS.2013.2293843

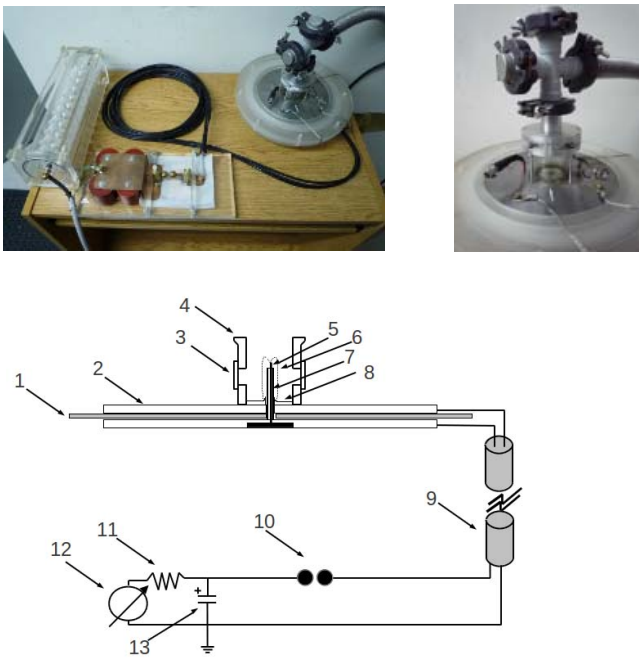


Fig. 1. Photo of the complete device (top left) and discharge chamber (top right). Below: PF schematic diagram: 1: PVDF insulator. 2: cathode plate. 3: borosilicate window. 4: discharge chamber. 5: anode. 6: artistic line simulating the current sheet. 7: Alumina insulator. 8: field intensifier. 9: transmission line. 10: spark gap. 11: charging resistor. 12: high-voltage source. 13: power source capacitor.

## II. Experimental Setup

The device was initially conceived in a cooperative research project between the National Nuclear Commissions of Argentina and Chile. Two similar devices were designed and build in each country. The Chilean device was named Nanofocus (not to be confused with the 100-J PF reported in [7]), and the Argentine device was called NanoPLADEMA. The work reported in this paper was conducted in the latter.

Essentially, these devices can be divided into three parts (Figs. 1 and 2): an energy source, a transmission line, and a discharge chamber. The source consists of a small (nF) capacitor ($C_1$), typically charged at several kilovolts, which is discharged through an adjustable length ($d$) air gap into three parallel 50-Ω coaxial cables several meters long forming a transmission line, and then into the discharge chamber consisting of two insulated metallic disks forming another capacitor $C_c$. The positive electrode of this capacitor contains the coaxial central electrode, separated from the second (grounded) capacitor plate by means of an alumina tube. The diameter and length of the central electrode are 2.0 and

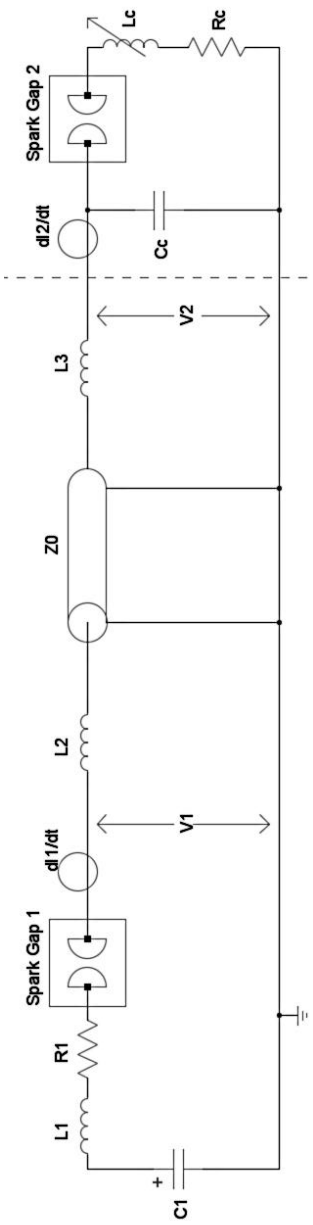


Fig. 2. Circuit diagram of the device nanoPLADEMA. The discharge chamber is shown at the right of the dashed line.

2.8 mm, respectively, and the outer diameter and length of the ceramic insulator are 4.0 and 2.3 mm, respectively. A small vacuum chamber is assembled on the ground plate, centered on the central electrode, which was evacuated down to a pressure of around 0.01 mbar. The chamber is then filled with hydrogen (or any convenient gas) at the desired pressure (in the millibar range). Fig. 2 shows a diagram of the equivalent electric circuit. The circuit has the following measured parameters: $C_1 = (5.4 \pm 0.1)$ nF, $C_c = (4.9 \pm 0.1)$ nF, coaxial lines length = 4.0 m.

In order to predict the circuit behavior, one could, in principle, simulate the complete equivalent circuit and then compare the calculated magnitudes (e.g., the discharge chamber current time derivative) with the measured ones. However, in view of the fact that there are too many unknown parameters ($L_1$, $L_2$, $L_3$, and $R_1$ in Fig. 2 and the closure details of the

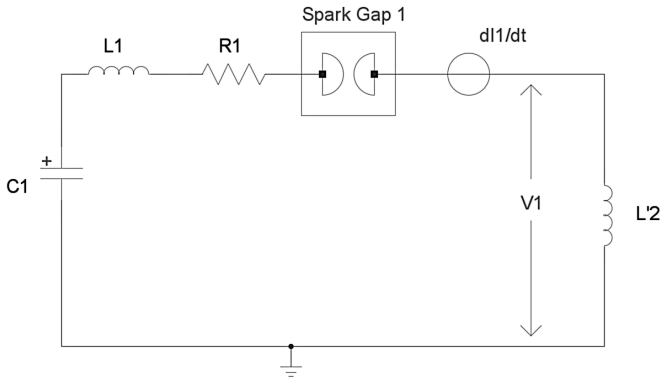


Fig. 3. Circuit diagram of the first configuration studied, where the transmission lines are replaced by a shortcircuit.

gaps), a piecewise analysis of the circuit was chosen as a better approach.

The first test case studied is a simple circuit which replaces the lines by a short-circuit (that is, a fixed inductance). The analysis of this configuration will provide information about $L_1$ and $R_1$, and also on the charging voltage dependence on the air-gap separation distance ($d$). The second study is performed by connecting the transmission lines but ending them in a short-circuit, which allows the determination of the value of $L_2$. In the third test, the transmission lines are connected to a 4-nF capacitor, which simulates the disk plates of the discharge chamber without the PF discharge and yields $L_3$. Finally, the complete system is analyzed using the previously obtained parameters. For each configuration described above, the device discharges were performed in a repetitive way (through simple self-breakdown of the gap), and it was verified that the electrical signals observed were substantially the same. In this paper, we show a representative dataset for each case.

A model of the concentrated parameters for the system in the different configurations was constructed and numerically simulated with Ngspice [8], a mixed-level/mixed-signal circuit simulator.

## III. Result

### A. Case 1: Transmission Lines Replaced by a Short-Circuit

Fig. 3 shows the equivalent circuit in which the transmission line was replaced by a short-circuit. With this configuration, several shots were fired at three different separations of the air-gap electrodes (i.e., $d = 1$, 2.7, and 4.5 mm). The maximum charging voltage ($V_0$) of $C_1$ in each case was 4.1, 9.1, and 16.0 kV, respectively. In every discharge, the time evolution of the voltage behind the spark gap, $V_1(t)$, was measured with a fast resistive voltage divider, and the current time derivative $dI_1/dt$ was measured with a Rogowski coil. The recorded traces were similar in all cases, and only varied in their amplitudes when varying the $d$ value. Fig. 4 shows typical signals of the current derivative $dI_1/dt$ and the voltage $V_1$ after the air gap, measured with $d = 2.7$ mm. It can be seen that, except for an initial stage, the curves correspond to damped sinusoids with the same period and damping in all the cases studied.

The numerical simulator was used to calculate $V_1$ and $dI_1/dt$. The voltage drop $V_{sg1}$ in the air gap was modeled

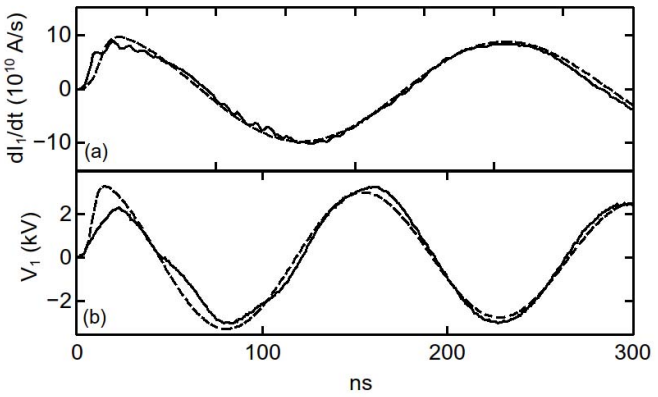


Fig. 4. Electric signals of a 9.1 kV discharge in the circuit shown in Fig. 3. Experimental measurements (solid line) and numerical simulations (dashed line).

as [9]

$$V_{sg1}(t) = V_0 \frac{2}{1+\exp\left(\frac{-4.4t}{\Delta t}\right)}. \quad (1)$$

The values of $L_1$, $L_2'$, $R_1$, and $\Delta t$ were adjusted to obtain a reasonable fit, which is shown by the dashed lines in Fig. 4. The resulting values are: $L_1 = (61 \pm 2)$ nH; $L_2' = (40 \pm 2)$ nH; $R_1 = 0.24 \pm 0.04\ \Omega$; and $\Delta t = 8$ ns. The same set of values was found for all the air-gap separations.

The initial portion of the signals presents oscillations with the same frequency but increasing amplitudes. This feature has already been reported by [9] and [10] and can be explained by the drop of the gap resistance below the required value to close the circuit in a time interval comparable with the discharge period. Although the full explanation of this effect is beyond the scope of this paper, the specifics of the present case require a comment. Note that, in order to close the circuit and get an oscillating behavior, the equivalent spark gap resistance $R_{sg}$ should satisfy

$$R_{sg} < 2\sqrt{\left(L_1 + L_2'\right)/C_1} \approx 9\ \Omega.$$

Assuming that the initial diameter of a spark in air at atmospheric pressure is about 0.1 mm [11], the resistance of forming a conducting channel of length $d$ in the air gap can be estimated as $R_{sg} = 4d\ 10^8/\sigma\pi$. When the ionization degree becomes larger than a few percent, the conductivity $\sigma$ depends only on the electron temperature $T_e$, i.e., $\sigma \sim 2760\ T_e^{3/2}\Omega \cdot$ m ($T_e$ in eV units). Since $T_e$ remains constant at about 2–3 eV until the completion of the ionization, for the smallest $d$ (1 mm) one can estimate $R_{sg} \sim 11.7\ \Omega$. Obviously, longer gaps should have larger resistances under the same conditions. Therefore, to close the gap in this circuit, additional electron heating (i.e., higher $T_e$) is required (which cannot happen before reaching full ionization of the channel) or, more likely, a diminution in $R_{sg}$ through radial expansion of the channel. The latter is indeed probable since the pressure of fully ionized and thermalized plasma at a few electronvolts and atmospheric density is about 200 times higher than that of the surrounding gas. Hence the channel should radially expand as a strong shock wave, doubling its diameter in about 20 ns. Therefore, if $T_e$ maintains or increases its value by Joule heating, $R_{sg}$ should diminish by at least a factor 4, which satisfies the closure condition. The minimum amount of energy required for forming a fully ionized and thermalized 1 mm channel is about 0.6 mJ, which is relatively small compared to the total energy in the capacitor (45 mJ at 4.1 kV). Larger gap separations entail higher initial $R_{sg}$ values but with larger charging voltages, which preclude longer closure times. In effect, [10] have shown that the time to fully ionize and heat the ions is independent of the air-gap separation $d$, and the power per unit length delivered to the plasma actually increases with $d$. In any case, the energy expended in closing the air gap is in the order a few percent of the total energy in this device, and even smaller in that used by the Chilean group.

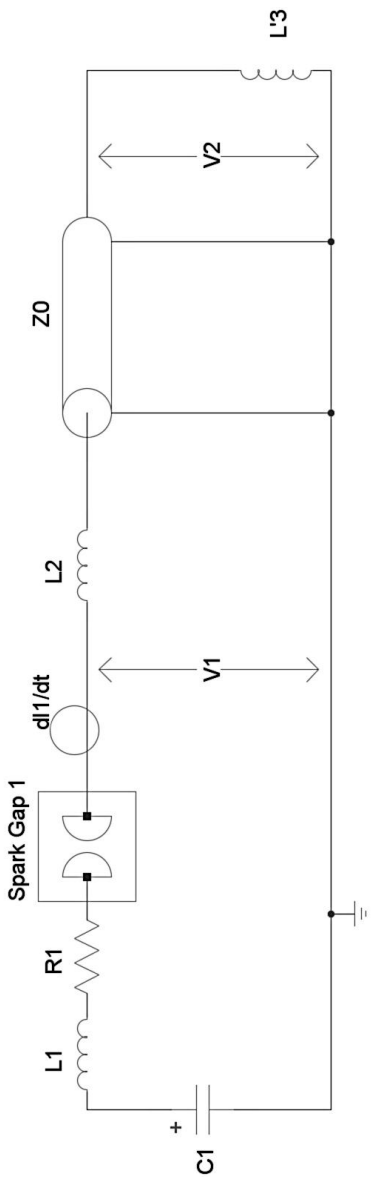


Fig. 5. Equivalent circuit of the system with a transmission line closed with a short-circuit.

### B. Case 2: Transmission Lines Ending in a Short-Circuit

In the second configuration, the transmission lines are short-circuited at its end (Fig. 5). The transmission line and its connections increase the inductance $L_2'$ measured in the first case.

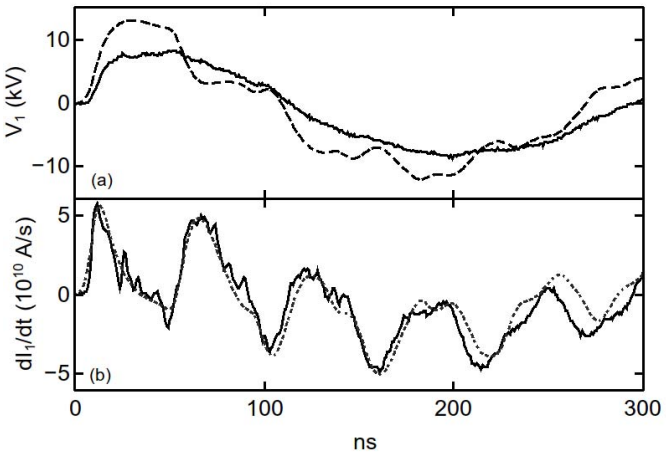


Fig. 6. Electric signals of a 16 kV discharge in the circuit shown in Fig. 5. Experimental measurements (solid line) and numerical simulations (dashed line).

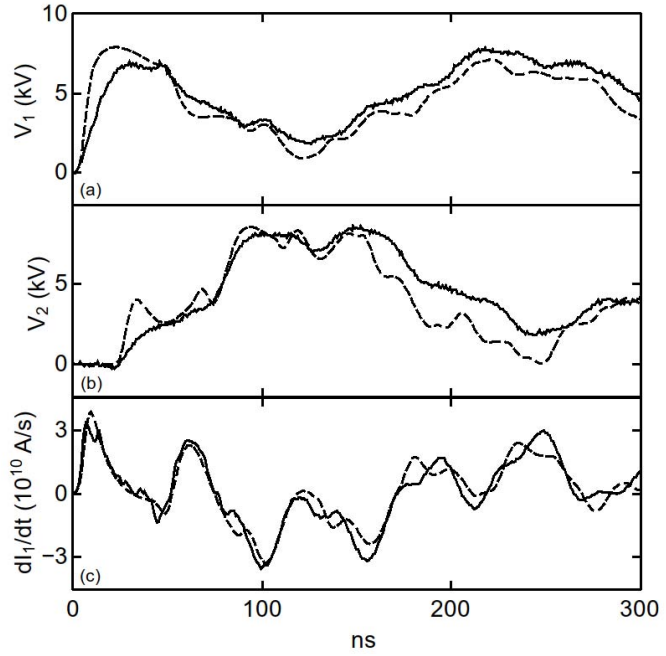


Fig. 7. Electric signals of a 9.1 kV discharge in the circuit shown in Fig. 5 with the transmission line ended in a 4 nF capacitor. Experimental measurements (solid line) and numerical simulations (dashed line).

The larger stray inductance in the second configuration, $L_2$, is the one needed for the final circuit. The short-circuited side of the line is modeled by an inductance $L_3'$. Fig. 6 shows the signals of the current derivative $dI_1/dt$ and the voltage after the air gap, $V_1$, measured with $d = 4.5$ mm. The dashed lines in Fig. 6 show the numerical simulation obtained. The transmission line was simulated using a single lossy transmission line (TXL) model. The values of $L_2$ and $L_3'$ that best fit the experimental signals are 90 and 60 nH, respectively. The values of $\Delta t$, $R_1$, and $L_1$ previously determined were used.

Additional measurements were performed in a circuit where the short-circuit was replaced by a 4-nF capacitor emulating the capacitor formed by the parallel plates of the chamber. Fig. 7 shows the current derivative $dI_1/dt$, the voltage after the air gap, $V_1$, and the voltage $V_2$ on the 4-nF capacitor, using a

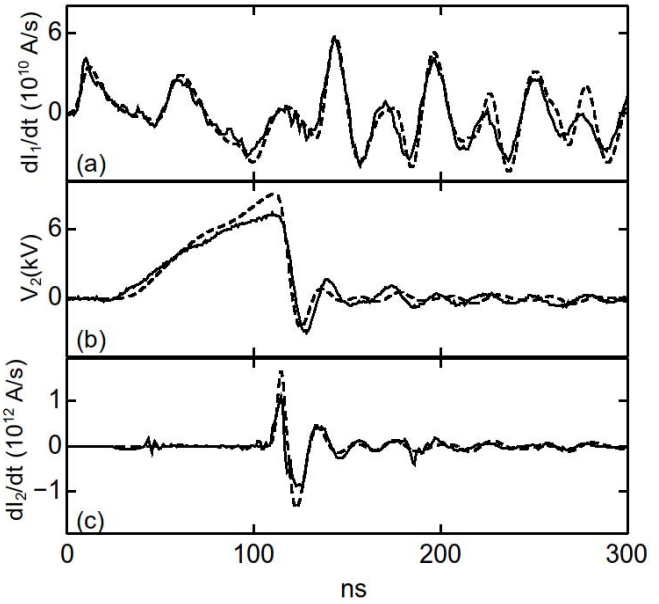


Fig. 8. Electric signals of a 9.1 kV discharge in the circuit shown in Fig. 2. The charging pressure in the PF chamber is 5 mbar. Experimental measurements (solid ine) and numerical simulations (dashed line).

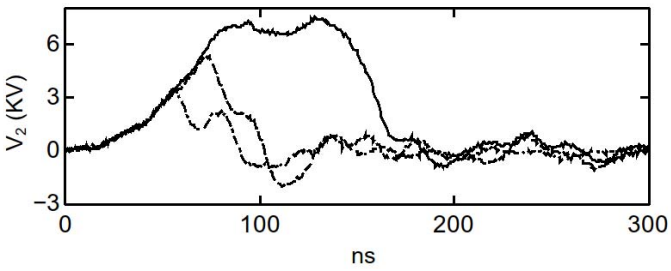


Fig. 9. Temporal evolution of $V_2$ for the circuit shown in Fig. 2 for different $H_2$ filling pressures 2 mbar (solid line), 10 mbar (dashed line) and 19 mbar (dash-dot line).

separation $d = 2.7$ mm in the gap. The dashed lines in Fig. 7 are the numerical simulations using the same set of parameters as in Fig. 6, except for $L_3'$, which was adjusted to 75 nH.

### C. Case 3: Complete System

Fig. 8 shows the experimental signals of $dI_1/dt$, $V_2$, and $dI_2/dt$, measured during a 9.1 kV discharge with the transmission line connected to the electrodes within the vacuum chamber filled with hydrogen at 5 mbar. The dashed lines in Fig. 8 are the corresponding numerical simulations of the circuit depicted in Fig. 2 assuming a constant $L_c$ value. The values of $R_1$, $L_1$, and $L_2$ are the same as before. The operation of the second spark gap (the breakdown in the chamber) was modeled as

$$V_{sg2}(t) = V_2(t)\ \frac{1+\exp\left(-\frac{4.4t_o}{\Delta t'}\right)}{1+\exp\left[\frac{4.4(t-t_o)}{\Delta t'}\right]} \tag{2}$$

which accounts for a time delay ($t_o$) between the closure of the air gap and the breakdown in the gas inside the chamber. The best fit of the experimental signals at 5 mbar corresponds to $t_o = 113$ ns, $\Delta t' = 5$ ns, $L_3 = 40$ nH, $R_c = 0.45\ \Omega$, and

$L_c = 2.5$ nH. From the analysis of other signals (see Fig. 9), $t_o$ showed an inverse dependence with the filling pressure, which is in agreement with previous experimental reports [12] on low-pressure gas breakdown.

## IV. Conclusion

A procedure for determining the parameters of the electrical circuit in a miniature PF device was characterized by means of a lumped numerical model calibrated with experimental diagnosis. It turns out that the plasma in the discharge chamber can be represented by a relatively small and constant value of inductance, at different filling pressures, when using a small length transmission line. Hence, in this device the voltage and current time derivative measurements are insufficient to determine the dynamics of the plasma. We must note here that the Chilean device has a 20-m transmission line and its behavior cannot be trivially extrapolated from our results.

Another relevant observation is the fact that the voltage at which the chamber disk capacitor is charged is clearly limited by the gas filling pressure inside the chamber and not just by the voltage in the capacitor energy source. This has stringent consequences on the energy delivered to the plasma in the chamber. Moreover, the present results suggest that the behavior of the discharge current within the vacuum chamber is likely to depend on the whole system and not only on the last portion of the circuit, even for longer transmission lines. How these facts affect the functioning of the device used at the Chilean Atomic Commission cannot be assessed with this paper and requires further studies.

## References


[1] J. Mather, *Dense Plasma Focus in Methods of Experimental Physics*, vol. 9. New York, NY, USA: Academia, 1971, pp. 187–221.

[2] M. Barbaglia, H. Bruzzone, H. Acuña, L. Soto, and A. Clausse, "Experimental study of the hard X-ray emissions in a plasma focus of hundreds of joules," *Plasma Phys. Control. Fusion*, vol. 51 no. 4, pp. 045001-1–045001-9, 2009.

[3] C. Pavez and L. Soto, "Demonstration of X-ray emission from an ultra-miniature pinch plasma focus discharge operating at 0.1 J nanofocus," *IEEE Trans. Plasma Sci.*, vol. 38, no. 5, pp. 1132–1135, May 2010.

[4] T. D. Butler, I. Henins, F. C. Jahoda, J. Marshall, and R. L. Morse, "Coaxial snowplow discharge," *Phys. Fluids*, vol. 12, no. 9, pp. 1904–1916, 1969.

[5] F. Gratton and M. Vargas, "Analytic solutions for the motion of the axial symmetric current sheath in a plasma focus," in *Proc. 7th Eur. Conf. Control. Fusion Plasma Phys.*, Lausanne, Switzerland, 1975, pp. 64–69.

[6] J. González, M. Barbaglia, F. Casanova, and A. Clausse, "A lumped parameter model of free expanding plasma focus," *Brazilian J Phys.*, vol. 39, pp. 633–637, 2009.

[7] M. Milanese, R. Moroso, and J. Pouzo, "D-D neutron yield in the 125 J dense plasma focus nanofocus," *Eur. Phys. J. D, Atomic, Molecular, Opt. Plasma Phys.*, vol. 27, no. 1, pp. 77–81, 2003.

[8] P. Nenzi and H. Vogt. (2011). *Ngspice Users Manual, Version 23* [Online]. Available: http://ngspice.sourceforge.net

[9] H. Bruzzone, H. Kelly, and C. Moreno, "On the effect of finite closure time of switches in electrical circuits with fast transient behavior," *Amer. J. Phys.*, vol. 57, no. 1, pp. 63–66, 1993.

[10] H. Bruzzone, C. Moreno, and R. Vieytes, "Measurement of the time evolution of averaged impedances in a small atmospheric pressure spark-gap," *Meas. Sci. Technol.*, vol. 4, no. 9, pp. 952–956, 1989.

[11] J. Meek and J. Craggs, *Electrical Breakdown of Gases*. Chichester, U.K.: Wiley, 1978.

[12] H. Bruzzone, H. Acuña, M. Barbaglia, and A. Clausse, "A simple plasma diagnostic based on processing the electrical signals from coaxial discharges," *Plasma Phys. Control. Fusion*, vol. 48, no. 5, pp. 609–620, May 2006.



**Mario Oscar Barbaglia** received the M.Sc. degree in electronic engineering from National Technological University, Regional Paraná, Argentina, in 1998, and the Ph.D. in engineering sciences from the Balseiro Institute, National University of Cuyo, Mendoza, Argentina, in 2003.

He is currently a Researcher with the National Scientific and Technical Research Council of Argentina and a Lecturer with the Physics Department, Faculty of Exact Sciences, National University of the Center, Buenos Aires, Argentina. His current research interests include pulse power, fusion devices, pulsed electromagnetic sources, and instrumentation.

**Horacio Bruzzone** received the M.Sc. and Ph.D. degrees in physics from the University of Buenos Aires, Buenos Aires, Argentina, in 1967 and 1976, respectively.

He was an Associate Professor of physics with the University of Buenos Aires, from 1981 to 1998, and he heads the Experimental Plasma Physics Group, Institute of Plasma Physics, Buenos Aires. Since 1999, he has been the Head of the Fast Pulsed Discharges Laboratory, University of Mar del Plata, Mar del Plata, Argentina. His current research interests include plasmas produced using fast pulsed discharges, with emphasis in plasma focus and Z-pinch devices.

Dr. Bruzzone is a fellow of the National Science and Technology Council of Argentina. He is currently a Chairman of the Scientific Committee for the International Centre on Dense Magnetized Plasmas, Poland.

**Hugo Néstor Acuña** received the M.Sc. degree in physics from La Plata University, La Plata, Argentina, in 1988, and the Ph.D. degree in experimental plasma physics from Mar del Plata University, Mar del Plata, Argentina, in 2001.

He is an Assistant Professor of basic physics. His current research interests include fast pulsed discharges in plasma focus and Z-pinch devices.

**Leopoldo Soto** received the B.S., M.S., and Ph.D. degrees in physics from Pontificia Universidad Católica de Chile, Santiago, Argentina, in 1989, 1990, and 1993, respectively.

He is the Head of the Thermonuclear Plasma Department of the Nuclear Chilean Energy Commission, CCHEN, and the Director of the Center for Research and Applications in Plasma Physics and Pulsed Power, P4 CCHEN-U, Talca. He is an Associate Professor of the Ph.D. Program in physics with the University of Concepción, Concepción, Chile, and the Ph.D. Program in applied science with the University of Talca, Talca, Chile, and an Associate Full Professor with Universidad Andres Bello, Departamento de Ciencias Físicas, Chile. He was the President of the Chilean Physical Society from 2003 to 2008. Currently, he is the Secretary General of the Chilean Physical Society from 2013 to 2015. His current research interests include dense transient plasmas, pulsed power and applied optics, including Z-pinch, plasma focus, capillary discharges, pulsed power miniature devices, transient plasma diagnostics, holography, interferometry, and optical refractive diagnostics.

Dr. Soto received the Presidential Chair in Science by the President of Chile in 1999. In 2007, he was a fellow of the Institute of Physics, U.K.

**Alejandro Clausse** received the Engineering and Ph.D. degrees from Instituto Balseiro, Bariloche, Argentina, in 1981 and 1986, respectively.

He is a Professor with the University of the Central Buenos Aires, Buenos Aires, Argentina, where he leads the Institute Pladema. He is a Principal Researcher with the National Science and Technology Council of Argentina, Argentina. His current research interests include plasma focus devices and its applications.